Supporting information for publication

Synthesis of Hexagonal Nanophases in the La_2O_3–MO_3 (M = Mo, W) Systems

E.D. Baldin[1], N.V. Lyskov[2,3], G.A. Vorobieva[1], I.V. Kolbanev[1], O.K. Karyagina[4], D.N. Stolbov[5], V.I. Voronkova[6], A.V. Shlyakhtina[1]

[1]*N.N. Semenov Federal Research Center for Chemical Physics, Russian Academy of Sciences, Moscow, Russia*

[2]*Federal Research Center of Problems of Chemical Physics and Medical Chemistry RAS, Moscow region, Chernogolovka, Russia*

[3]*National Research University "Higher School of Economics," Moscow, Russia*

[4]*Emanuel Institute of Biochemical Physics RAS, Moscow, Russian Academy of Sciences, Russia*

[5]*Department of Chemistry, Lomonosov Moscow State University, Moscow, Russia*

[6]*Department of Physics, Lomonosov Moscow State University, Moscow, Russia*

Table S1. Comparison of the refinement factors (R_{exp}, R_{wp}, R_p, χ^2) for different models used in the Rietveld refinement of the XRD patterns obtained in the La_2O_3+WO_3 mechanically activated oxide mixture with different thermal prehistory.

Composition of the starting mixture	Thermal history	Single-phase model $La_{18}W_{10}O_{57}$	Two-phase model $La_{18}W_{10}O_{57}$+La_2O_3
La_2O_3:WO_3	Heating in a DSC cell at 10 °C/min to 760 °C	Rwp 15.37% Rp 12.40% S 1.6724 χ^2 2.7970	Rwp 15.54% Rp 12.57% S 1.6807 χ^2 2.8247 La_2O_3 2.03(15) wt.%
	Heating of a green compact to 800 °C (6 h)	Rwp 14.55% Rp 11.56% S 1.6567 χ^2 2.7446	Rwp, % 14.24 Rp, % 11.46 S 1.6186 χ^2 2.6199 La_2O_3 4.14(13) wt.%

	Heating of a green compact to 900 °C (6 h)	Rwp 15.08% Rp 11.50% S 1.5757 χ^2 2.4828	Rwp, % 17.05 Rp, % 13.41 S 1.7800 χ^2 3.1683 La_2O_3 6.08(17) wt.%

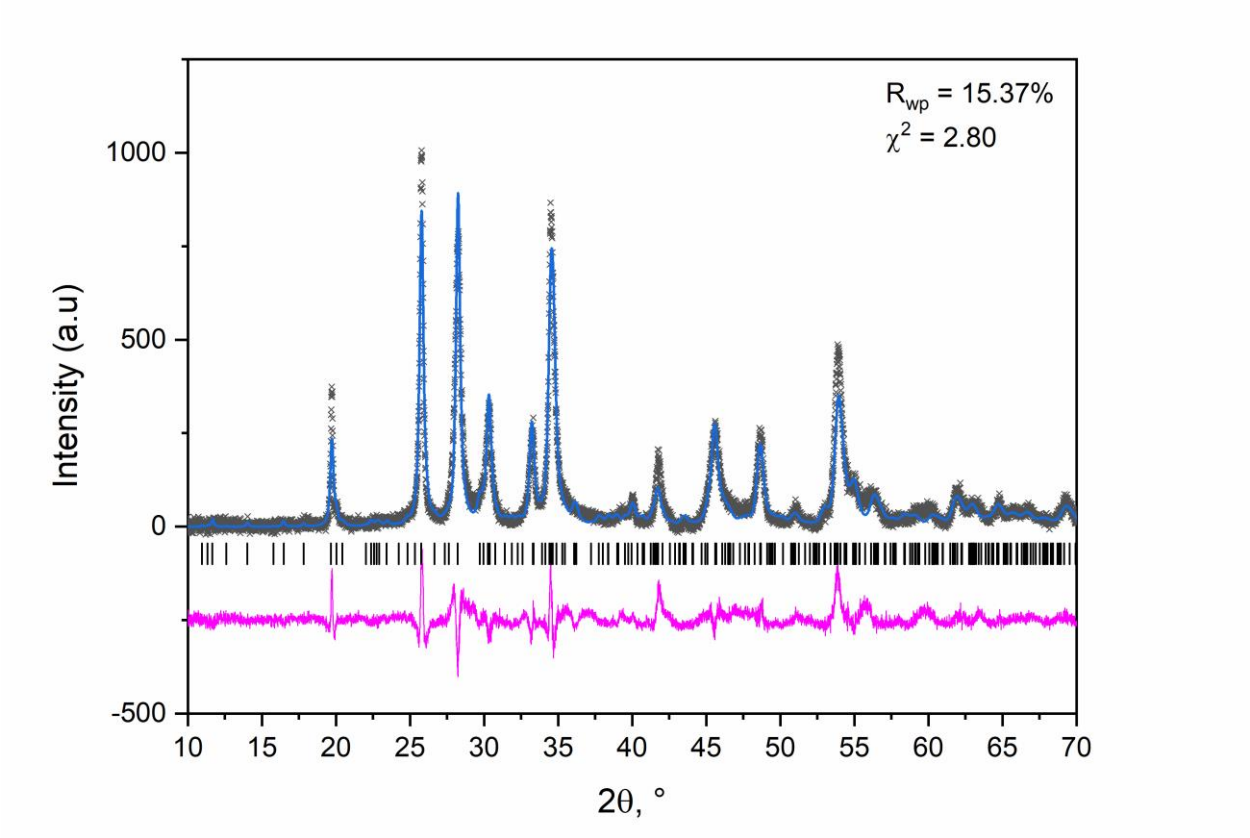

Figure S1. Rietveld refinement of the XRD pattern of the m/a La_2O_3+WO_3 mixture after heating to 760 °C. Crosses represent the observed pattern; the solid line through the symbols shows the calculated fit. Vertical bars mark the peak positions. The difference between the observed and calculated data is shown at the bottom.

Table S2. Comparison of the refinement factors (R_{exp}, R_{wp}, R_p, χ^2) for different models used in the Rietveld refinement of the hexagonal samples under consideration. The best models are highlighted in bold.

Composition and thermal history	I polytype $La_{18}W_{10}O_{57}$ Sp. gr. 190 P-62c	II polytype $La_{15}W_{8.5}O_{48}$ Sp. gr. 150 P321
$9La_2O_3{:}10WO_3$ 1400 °C, 4h	**Rwp, % 9.27** **Rp, % 7.36** **S 1.1527** **χ^2 1.3287**	Rwp, % 24.40 Rp, % 16.73 S 3.0419 χ^2 9.2530
$La_2O_3{:}WO_3$ 800 °C, 4h	Rwp, % 14.12 Rp, % 11.27 S 1.9361 χ^2 3.7484	**Rwp, % 13.12** **Rp, % 10.27** **S 1.7958** **χ^2 3.2247**
$La_2O_3{:}MoO_3$ 600 °C, 4h	Rwp, % 17.29 Rp, % 13.06 S 2.2566 χ^2 5.0924	**Rwp, % 13.30** **Rp, % 9.67** **S 1.7414** **χ^2 3.0324**

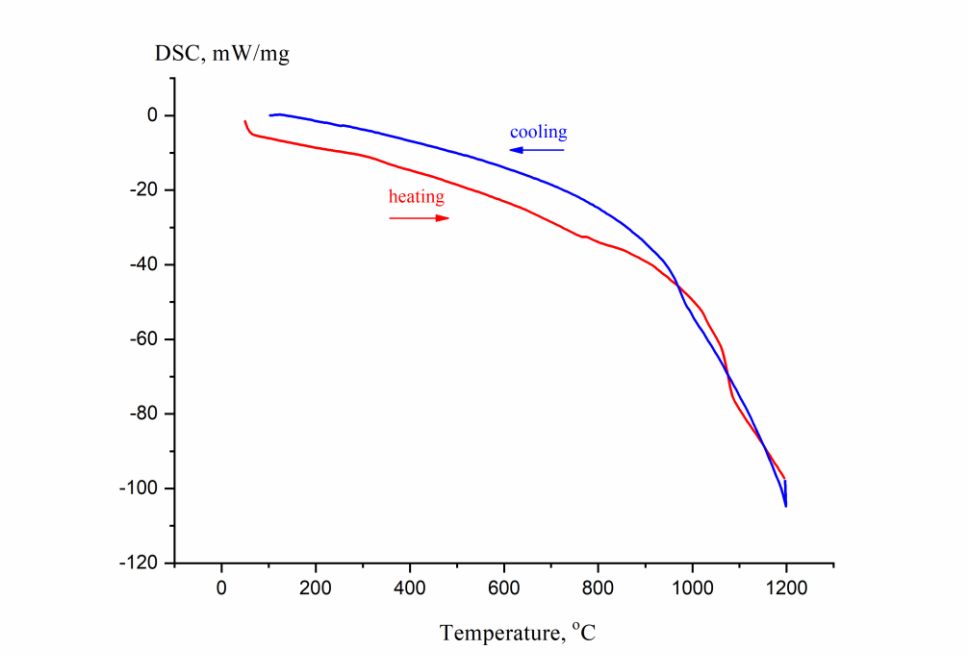

Figure S2a. Data were obtained in a DSC cell during heating to 1200 °C and cooling for powder of nanocrystalline hexagonal $La_{15}W_{8.5}O_{48}$ (phase II polytype 5H) prepared as an intermediate phase by firing a mechanically activated La_2O_3 + WO_3 starting mixture at 800 °C for 6 h.

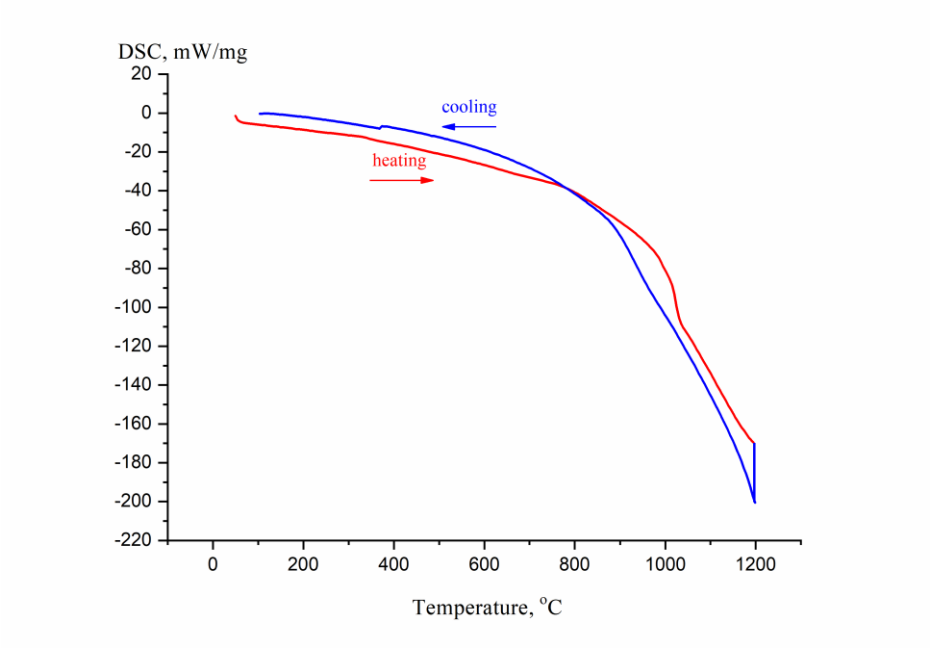

Figure S2b. Data were obtained in a DSC cell during heating to 1200 °C and cooling for powder of the coarse-grained hexagonal $La_{18}W_{10}O_{57}$ ceramic prepared by firing a mechanically activated $9La_2O_3 + 10WO_3$ starting mixture at 1400 °C for 4 h.

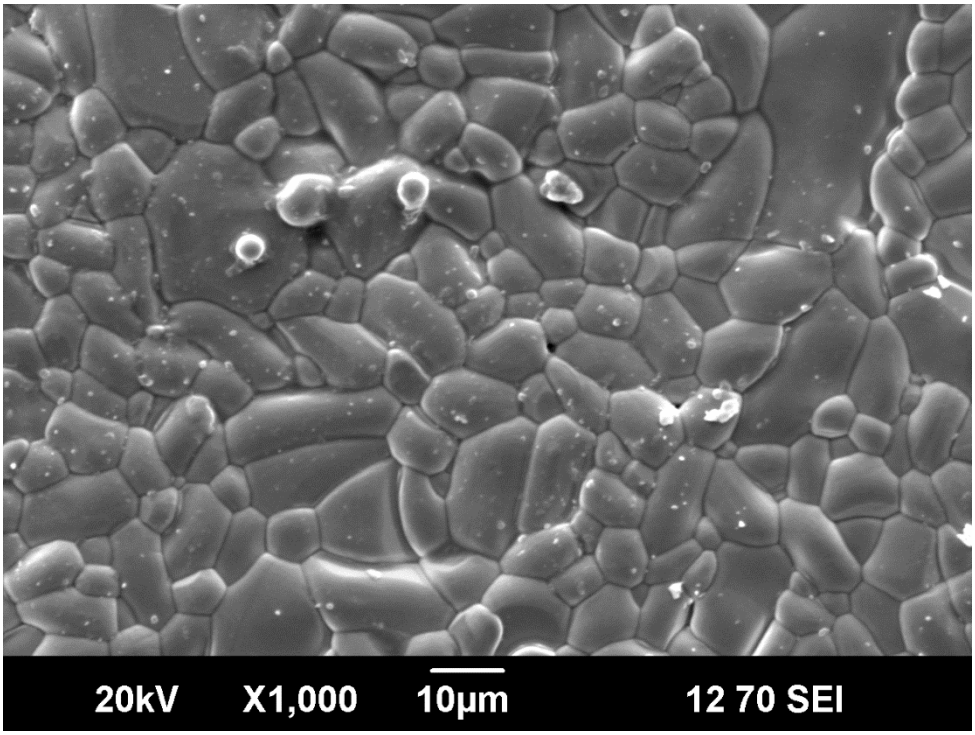

Figure S3. Microstructure of coarse-grained ceramics $La_{18}W_{10}O_{57}$ synthesized at 1400 ºC for 4 h.

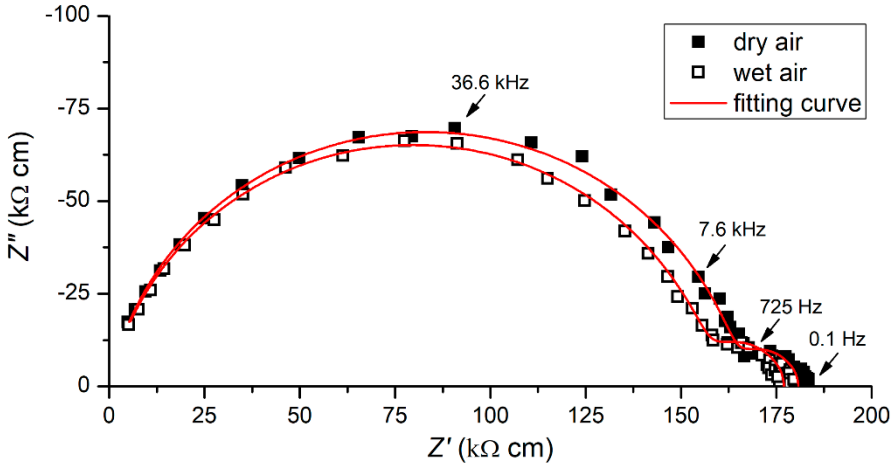

Figure S4a. 700 °C impedance spectrum of the $La_{15}W_{8.5}O_{48}$ nanoceramic obtained as an intermediate phase by firing a mechanically activated La_2O_3 + WO_3 starting mixture at 800 °C for 6 h.

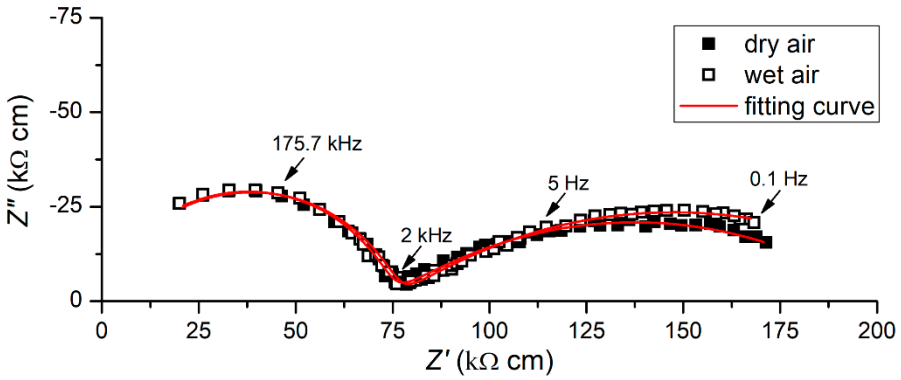

Figure S4b. 700 °C impedance spectrum of the coarse-grained hexagonal $La_{18}W_{10}O_{57}$ ceramic produced by firing a mechanically activated $9La_2O_3$ + $10WO_3$ starting mixture at 1400 °C for 4 h.

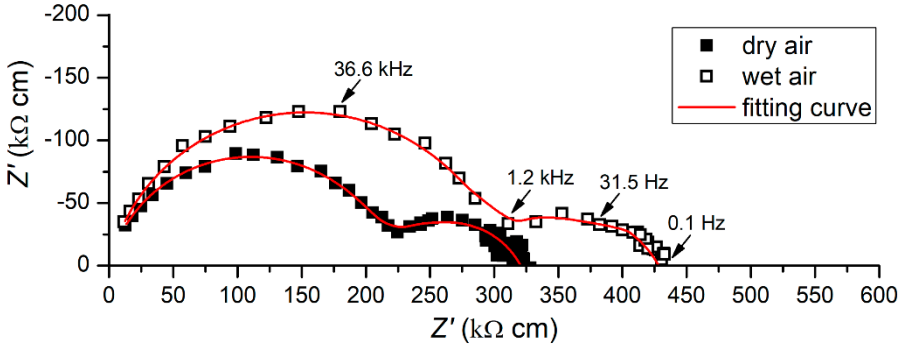

Figure S4c. 700 °C impedance spectrum of the $La_{15}Mo_{8.5}O_{48}$ nanoceramic obtained as an intermediate phase by firing a mechanically activated La_2O_3 + MoO_3 starting mixture at 800 °C for 6 h.

The impedance responses obtained have the form of two arcs of a circle: one at high frequencies (1 to 500 kHz) and the other at medium and low frequencies (1 kHz to 0.1 Hz). The impedance spectra shown in Figures S4a and S4c were fitted with the equivalent electrical circuit (EEC) shown in Fig. S4d(a). The EEC consists of two parallel circuits containing a resistor and a constant phase element (R_b-CPE_b, R_{gb}-CPE_{gb}). The impedance of *CPE* can be expressed as

$$Z_{CPE} = \frac{1}{A \cdot (j\omega)^P}, \qquad (1)$$

where A is a proportionality factor and the exponent P is related to the phase angle. The first arc corresponds to the impedance response related to the bulk resistance (R_b) of the sample. Note that the center of the arc is slightly depressed relative to the real axis; the exponent P is 0.87–0.91. The specific capacitance corresponding to the bulk impedance part was ~10^{-11} F cm^{-1}. The second arc is the response related to the grain-boundary resistance (R_{gb}) of the sample, as its characteristic capacitance is ~10^{-8} F cm^{-1}. Note that there is no electrode dispersion in the low-frequency limit. The total resistance of the sample, which was used to calculate conductivity (σ), was determined as the sum of R_b and R_{gb}.

The nature of the impedance response shown in Figure S4b is slightly different from the spectra shown in Figures S4a and S4c. In this case, the impedance response also combines two arcs. The high-frequency arc (1 to 500 kHz) corresponds to the contribution of the bulk resistance (R_b) of the sample. In comparison, the arc corresponding to the medium and low-frequency range (1 kHz to 0.1 Hz) is due to the electrode polarization (R_p). In this case, an equivalent circuit shown in Fig. 4d(b) was used to fit the impedance spectra, which also consisted of two parallel circuits containing a resistor and a constant phase element (R_b-CPE_b, R_p-CPE_p). The center of the high-frequency arc was slightly depressed relative to the real axis; the exponent P was 0.85–0.95. The specific capacitances corresponding to the bulk and electrode impedance parts were ~10^{-10}–10^{-11} F cm^{-1} and ~10^{-5} F cm^{-1}, respectively. The total resistance of the sample corresponded to the R_b value, which was used to calculate the conductivity (σ).

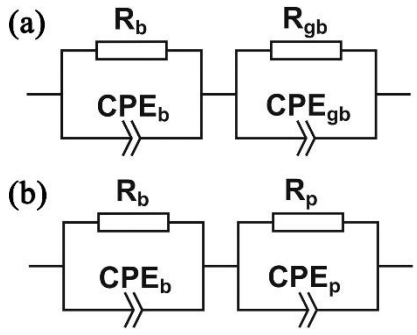

Figure S4d. An equivalent electrical circuit was used to fit the impedance spectra shown: (a) Figures S4a and S4c; (b) Figure S4b.

Table S3. Density of the low-density ceramics under study.

Composition and thermal history.	**Geometric density g/cm^3**	**Theoretical density g/cm^3**	**Relative density %**
La_2O_3:WO_3 800 °C, 4h	4.63	7.72	60.0
La_2O_3:WO_3 1000 °C, 6h	5.01	**Orthorhombic phase** 83.3 wt.% 7.44 **Hexagonal phase** 16.7 wt.% 7.62 **Total** 7.47	67.1
La_2O_3:MoO_3 600 °C, 4h	4.06	6.26	64.8
La_2O_3:MoO_3 900 °C, 4h	4.03	5.79	69.6

The total density was calculated using the following formula: $\rho_{total} = \frac{\rho_1\rho_2}{\rho_2\omega_1+\rho_1\omega_2}$

The program Smartlab Studio II generated a CIF file after Rietveld's refinement of the sample $La_{18}W_{10}O_{57}$ obtained after firing the $9La_2O_3$+$10MoO_3$ m/a mixture at 1400 °C for 4 h.

1625 I polytype.cif